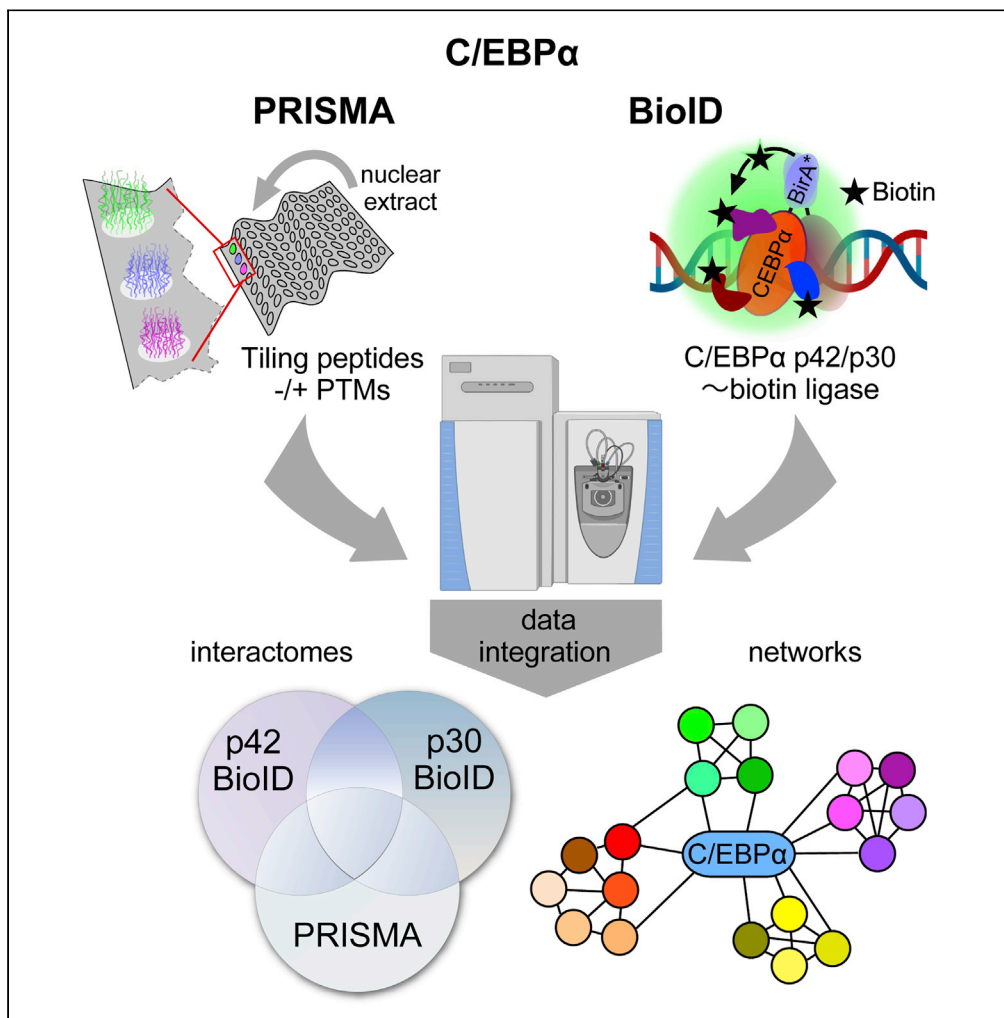


Article

PRISMA and BioID disclose a motifs-based interactome of the intrinsically disordered transcription factor C/EBP α



Evelyn Ramberger, Valeria Sapozhnikova, Elisabeth Kowenz-Leutz, ..., Philipp Mertins, Gunnar Dittmar, Achim Leutz

aleutz@mdc-berlin.de

Highlights

Combining peptide arrays and BioID refines the C/EBP α interactome

Hotspots of protein interactions in C/EBP α mostly occur in conserved regions

The interaction with the BAF/SWI-SNF complex is modulated by C/EBP α methylation

Experimental design suits interactome studies of intrinsically disordered proteins

Ramberger et al., iScience 24, 102686
June 25, 2021 © 2021
<https://doi.org/10.1016/j.isci.2021.102686>



Article

PRISMA and BioID disclose
a motifs-based interactome of the intrinsically
disordered transcription factor C/EBP α

Evelyn Ramberger,¹ Valeria Sapozhnikova,¹ Elisabeth Kowenz-Leutz,¹ Karin Zimmermann,¹ Nathalie Nicot,² Petr V. Nazarov,² Daniel Perez-Hernandez,^{1,2} Ulf Reimer,³ Philipp Mertins,¹ Gunnar Dittmar,^{1,2} and Achim Leutz^{1,4,5,*}

SUMMARY

C/EBP α represents a paradigm intrinsically disordered transcription factor containing short linear motifs and post-translational modifications (PTM). Unraveling C/EBP α protein interaction networks is a prerequisite for understanding the multi-modal functions of C/EBP α in hematopoiesis and leukemia. Here, we combined arrayed peptide matrix screening (PRISMA) with BioID to generate an *in vivo* validated and isoform specific interaction map of C/EBP α . The myeloid C/EBP α interactome comprises promiscuous and PTM-regulated interactions with protein machineries involved in gene expression, epigenetics, genome organization, DNA replication, RNA processing, and nuclear transport. C/EBP α interaction hotspots coincide with homologous conserved regions of the C/EBP family that also score as molecular recognition features. PTMs alter the interaction spectrum of C/EBP-motifs to configure a multi-valent transcription factor hub that interacts with multiple co-regulatory components, including BAF/SWI-SNF or Mediator complexes. Combining PRISMA and BioID is a powerful strategy to systematically explore the PTM-regulated interactomes of intrinsically disordered transcription factors.

INTRODUCTION

CCAAT enhancer binding protein alpha (C/EBP α) is a lineage instructing pioneering transcription factor involved in cell fate decisions in various cell types, including myeloid cells, adipocytes, hepatocytes, and skin cells. In myelopoiesis, C/EBP α cooperates with other transcription factors and chromatin modifying enzymes to regulate hematopoietic stem cell biology, lineage choice and expression of myeloid genes (Avelino and Delwel, 2017; Zaret and Carroll, 2011). Knockout experiments in mice show that C/EBP α regulates hematopoietic stem cell functions and that its removal blocks progenitor differentiation at the myeloid commitment stage (Bereshchenko et al., 2009; Kirstetter et al., 2008a; Zhang et al., 2004). The intronless *CEBPA* gene is mutated in approximately 10-15% of human acute myeloid leukemia (AML) cases. Mutations located within the N-terminal part of the gene obstruct expression of the full-length isoform p42 C/EBP α and favor expression of the N-terminally truncated isoform p30 C/EBP α (Fasan et al., 2014; Lin et al., 2005; Pabst et al., 2001). Experimental hematology and targeted mouse genetics have demonstrated that p30 C/EBP α represents a highly penetrant AML driver oncoprotein (Bereshchenko et al., 2009; Kirstetter et al., 2008b).

Unraveling the protein interaction network of C/EBP α in hematopoietic cells is a prerequisite for the understanding of diverse gene regulatory and epigenetic functions of C/EBP α in normal hematopoiesis and AML. Previous research has shown that the N-terminus of vertebrate C/EBP α harbors short, conserved regions (CRs) that function in a modular and combinatorial fashion to regulate gene expression (Leutz et al., 2011; Tsukada et al., 2011). The N-terminally truncated, leukemogenic p30 C/EBP α isoform contains only one of the transactivation modules (CR1L, TEIII). P30 C/EBP α retains residual gene regulatory and epigenetic capacity to direct myeloid lineage commitment but lacks the cell maturation inducing and proliferation restricting functions of the long C/EBP α isoform p42 (Bereshchenko et al., 2009; Pedersen et al., 2001). Only the C-terminal part of C/EBP α , comprising approximately one-quarter of the protein, may adopt a structured basic leucine zipper (bZIP) domain upon binding to DNA target sites (Seldeen et al., 2008). Otherwise, C/EBP α and family members, but also many other transcription factors contain several

¹Max Delbrück Center for Molecular Medicine in the Helmholtz Association, Robert-Rössle-Strasse 10, 13125 Berlin, Germany

²Quantitative Biology Unit, Luxembourg Institute of Health, 1a Rue Thomas Edison, 1445 Strassen, Luxembourg

³JPT Peptide Technologies GmbH, Volmerstrasse 5, 12489 Berlin, Germany

⁴Institute of Biology, Humboldt University of Berlin, 10115 Berlin, Germany

⁵Lead contact

*Correspondence: aleutz@mdc-berlin.de

<https://doi.org/10.1016/j.isci.2021.102686>



intrinsically disordered regions (IDRs), short linear motifs (SLiM) and molecular recognition features (MoRF). These are typical hallmarks of gene regulatory proteins that integrate signal transmission, gene regulation, and epigenetic regulation through promiscuous interactomes (Dunker et al., 2002; Dyson and Wright, 2005; Tompa, 2012; Uversky et al., 2005; van der Lee et al., 2014; Ward et al., 2004; Wright and Dyson, 1999). PTMs, downstream of signaling cascades, frequently alter dynamic protein interaction interfaces of IDR/SLiM/MoRF modules and are of high biological relevance but remain difficult to capture with traditional immune affinity-based methods because of their transient nature, weak affinity, and/or sub-stoichiometric participation in biomolecular condensates (Perkins et al., 2010; Sabari et al., 2020).

Within the C/EBP family, mutation of PTM sites, including phosphorylation (S, T, Y residues), methylation (K, R residues), and acetylation sites (K residues) or deletion of CRs in their N-termini may radically alter their biological functions (Leutz et al., 2011). Assessment of the known C/EBP α interactome data showed a surprisingly low overlap (less than 5%) between various published immuno-affinity-mass spectrometry (MS) datasets, hampering the deduction of C/EBP α functions and adjunct molecular mechanisms (Cirilli et al., 2017; Giamb Bruno et al., 2013; Grebien et al., 2016). Here, we combined the protein interaction screen using a peptide matrix (PRISMA) method (Dittmar et al., 2019) with biotin proximity labeling identification (BioID) (Roux et al., 2012) to match high confidence interactomes across the amino acid sequence and PTM sites with the p42/p30 C/EBP α isoforms in living myeloblastic cells. This experimental strategy may be adapted to explore other multi-valent intrinsically disordered transcriptional regulators, many of which are involved in development and disease.

RESULTS

Mapping the C/EBP α interactome with PRISMA

We have previously established the PRISMA method to explore the linear interactomes of intrinsically disordered proteins and applied it to C/EBP β and its PTMs (Dittmar et al., 2019). Here, we slightly modified the PRISMA protocol to explore the linear and PTM-dependent C/EBP α interactome. Briefly, 15 amino acid long peptides covering the amino acid sequence of C/EBP α in a tiling fashion were spot-synthesized on a membrane support. The peptide membrane was incubated with nuclear extracts derived from the human promyelocytic leukemia cell line, NB4, and bound proteins of each spot were subsequently analyzed using quantitative mass spectrometry (Figure 1A). The C/EBP α peptide array included 114 peptides with and without PTMs that were designed with a sequence overlap of seven amino acids (Tables S1 and S2). The overall technical reproducibility of the PRISMA screen replicates showed a median Pearson correlation coefficient of 0.85 and discrete patterns of correlation between different C/EBP α regions (Figure S1). PRISMA detected a total of 2,274 proteins, of which 785 proteins passed the significance threshold (FDR <0.1) in at least one peptide spot (Figure 2B, Table S3). The majority of significant protein interactions were observed with peptides spanning AA 1-15 (CR2), AA 50-85 (part of CR3 and CR4) and AA 134-148 (part of CR1L) (Table S2). Together, C/EBP α regions CR2, CR3, CR4 and CR1L correspond to subdivisions of previously identified trans-regulatory regions with high sequence conservation between species and C/EBP factors (Leutz et al., 2011). Extracted binding profiles, as shown in Figure 2C, highlight distinct interaction profiles of selected protein complexes such as Mediator, or BAF/SWI-SNF components, previously shown to interact with C/EBP α .

The mediator of transcription complex (MED) is an essential transcriptional coactivator in eukaryotes that interacts with RNA Pol II and many transcription factors and co-factors. PRISMA revealed 17 MED proteins with similar binding patterns with dominant peaks in C/EBP α peptides corresponding to CR2,3,4 and CR1L. This finding suggests that the MED-complex interacts with multiple CRs in the N-terminus of p42 C/EBP α and with CR1L/TEIII, which corresponds to the N-terminus of p30 C/EBP α . The acetyltransferases, CBP/p300 (KAT3A/KAT3B), most strongly bound to peptides spanning regions CR3,4 with residual binding in CR2 and CR1L. Interaction with the chromatin remodeling BAF/SWI-SNF complex is essential for the anti-proliferative and differentiation functions of C/EBP α and has been previously found to require CR1L/TEIII in addition to the N-terminus of p42 C/EBP α (Muller et al., 2004; Pedersen et al., 2001). In PRISMA, BAF/SWI-SNF subunits bound to peptides corresponding to CR1L and CR3,4.

C/EBP proteins are extensively decorated with PTMs that may alter their interactome to direct their function (Kowenz-Leutz et al., 2010; Leutz et al., 2011). Of particular interest are a number of C/EBP-family member specific arginine residues, several of which have been shown in C/EBP β to be targets of mono- and dimethylation, with their mutation profoundly changing C/EBP β biology (Dittmar et al., 2019; Leutz et al., 2011). We examined C/EBP α for PTMs by mass spectrometry and discovered several known and novel methylation sites, including methylation of R12, R35 and R156 and further identified R142 (CR1L) by a

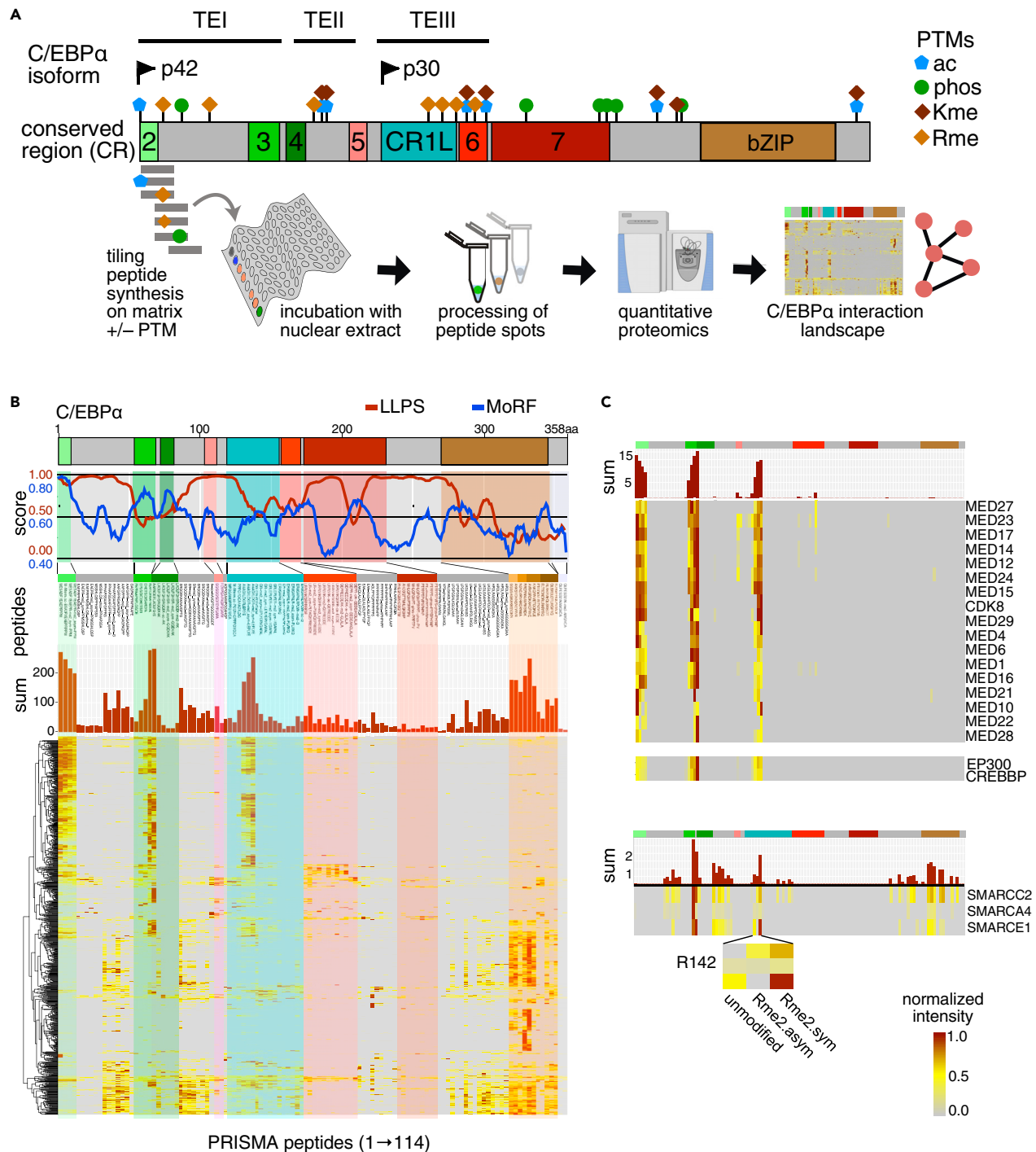


Figure 1. PRISMA delineates the linear interactome of CEBPA across conserved regions and PTM sites

(A) Schematic scaled depiction of CEBPA conserved regions (CRs) and post-translational modification (PTM) sites. The overlap of CRs with transactivating elements (TE) is indicated. Spot synthesized, immobilized peptides with and without PTMs covering the complete amino acid sequence of CEBPA were screened for protein interactions with PRISMA (n = 2).

(B) Line plots show liquid-liquid phase separation (LLPS; <http://protodyn-fuzpred.org>) and molecular recognition feature prediction (MoRF; <https://morf.msl.ubc.ca/index.xhtml>) across the CEBPA sequence. Heatmap shows the binding profile of all significant proteins (y-axis) across CEBPA PRISMA peptides ordered from N- to C-terminus (x-axis). Bar plot on top corresponds to the summed normalized LFQ intensities of all significant proteins in each peptide spot.

(C) Extracted CEBPA PRISMA profiles of Mediator and P300 complex (top) and BAF/SWI-SNF complex (bottom) subunits.

See also [Figures S1](#) and [S2](#), [Tables S1](#), [S2](#), and [S3](#).

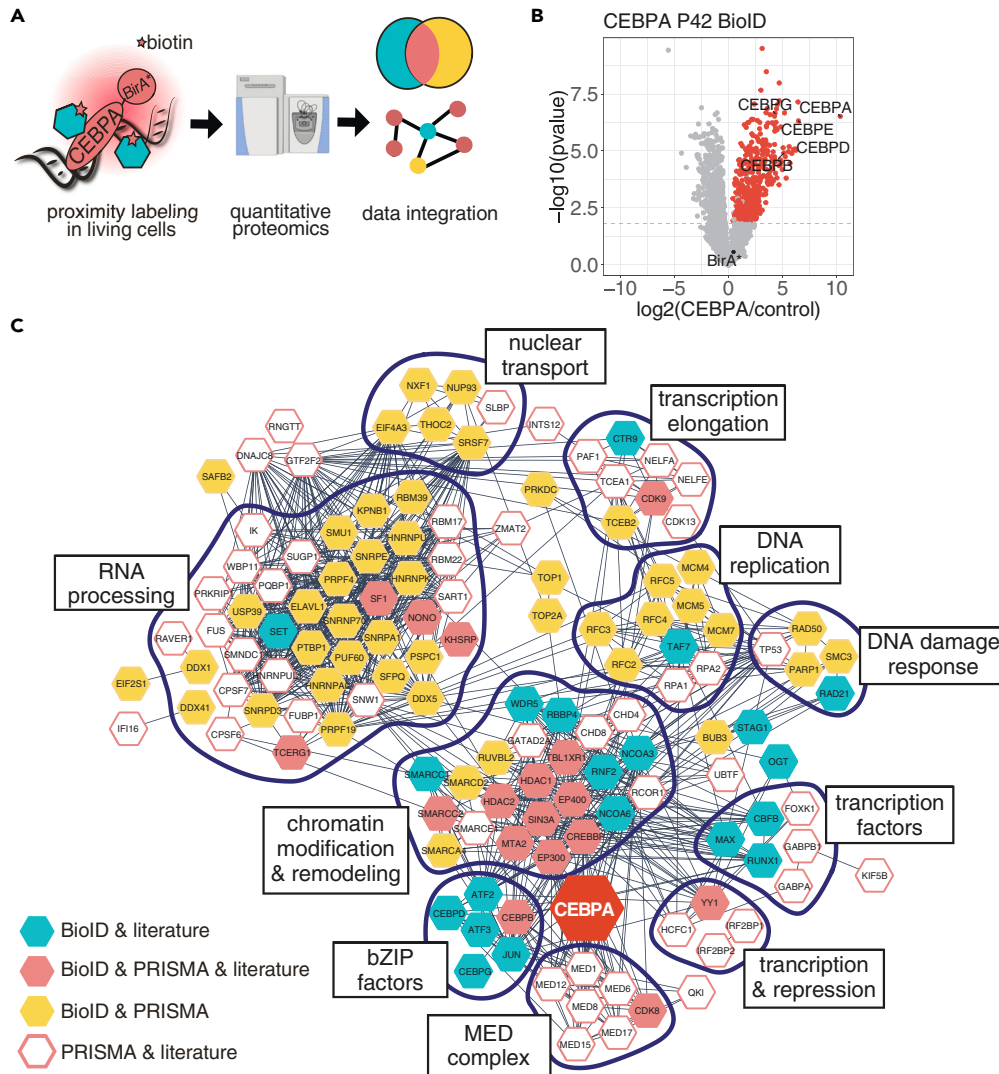


Figure 2. Integration of BioID and PRISMA data revealed a spatial CEBPA interactome with high interconnectivity

(A) BioID proximity labeling data obtained in living cells was integrated with biochemical data obtained with PRISMA.

(B) The CEBPA BioID interactome in NB4 cells. Log fold changes (CEBPA/control) of proteins are plotted against their p-values (student t-test, $n = 4$). The FDR cutoff (0.05) is indicated with a dotted line.

(C) Integrated protein interaction network of CEBPA. Color of nodes corresponds to detection in datasets as depicted in the legend. Edges represent validated protein interactions retrieved from the STRING database. Interactors not connected by any edges were removed from the plot (12 proteins). See also [Figures S3 and S4](#), [Table S4](#).

targeted MS-parallel reaction monitoring approach as a novel methylation site ([Figure S2](#)). The PRISMA data suggested increased binding of the BAF/SWI-SNF subunit SMARCE1 to R142 methylated peptides, as compared to the unmodified counterpart. Other subunits of BAF/SWI-SNF (SMARCA4, SMARCC2) followed a similar trend but their differential binding to the methylated peptide spanning R142 scored somewhat below the threshold set of statistical significance.

Given the sequence conservation between C/EBP proteins, we compared the PRISMA derived interactome of C/EBP α with the previously published C/EBP β PRISMA interactome ([Dittmar et al., 2019](#)). Despite some sequence differences in homologous regions and peptides, several shared interactors were identified. For example, the mediator complex was found to bind to the same homologue CRs in both proteins ([Figure S3](#)), confirming the functional similarity of these regions within the C/EBP family ([Jones et al., 2002](#)).

Cross-validation of PRISMA and BioID-C/EBP α interactomes

Next, we compared the interactomes derived from PRISMA and BioID proximity labeling data to generate a myeloid live cell validated linear C/EBP α interactome (Figure 2A). Briefly, NB4 cells were transduced with a Tet-On inducible lentiviral construct encoding a promiscuous biotin ligase (BirA*) fused to the C-terminus of C/EBP α . As controls, we used non-induced NB4 C/EBP α -BirA* cells or cells expressing only the ligase moiety (NB4 BirA*). Proximity labeling identified 397 C/EBP α proximal interactors (FDR <0.05). Among the most enriched proteins were several transcription factors of the C/EBP and ATF families, representing known heterodimerization partners of C/EBP α (Tsukada et al., 2011) and thus confirming successful BioID labeling (Figure 2B, Table S4).

In total, 88 proteins overlapped between the PRISMA and BioID derived C/EBP α interactomes of which 21 were previously identified interactors, including members of chromatin remodeling and histone acetylation/deacetylation complexes. In addition, 49 proteins significant in PRISMA and 26 proteins significant in BioID have been previously described to interact with C/EBP α (Chatr-Aryamontri et al., 2017; Grebien et al., 2016; Szklarczyk et al., 2015). Taken together, 137 proteins represent the subset of myeloid C/EBP α interactors with the highest confidence that can be depicted across the linear C/EBP α sequence +/- PTM sites. These interactors show high connectivity according to experimentally validated interactions listed in the STRING database (Figure 2C). Using the spatial information provided by PRISMA, we could also reveal distinct functional roles of individual CRs including chromatin remodeling (CR3,4; CR1L; bZIP), transcriptional regulation (CR2; CR3,4; CR1L; CR6; bZIP), and hematopoietic progenitor cell differentiation (CR3,4) (Figure S4, Table S5). CR3,4 is of particular interest since it contains most of the significantly enriched GO terms, confirming the importance of the core transactivating region of p42 C/EBP α . Although several proteins interacted with CR7, no GO terms were enriched with this region, pointing toward functional heterogeneity.

Arginine methylation-dependent interaction of BAF/SWI-SNF complex subunits

Differential interactions with post-translationally modified peptides in the primary C/EBP α sequence were also detected by PRISMA. Among them was the BAF/SWI-SNF complex that has been previously described to interact with C/EBP α (Pedersen et al., 2001). PRISMA revealed that the interaction with the SMARCE1 component is modulated by the newly discovered arginine methylation site R142 within CR1L/TEIII (Figure 3A). Accordingly, we performed BioID with an R142/149/156 to L142/149/156 mutant (triple R to L mutation; tR>L) of C/EBP α to examine the PTM-dependent BAF/SWI-SNF interaction in more detail. In accordance with the PRISMA results, SMARCE1 and three additional BAF/SWI-SNF subunits (ARID1A, ARID1B, ARID2) were significantly enriched in the p30 C/EBP α -tR>L mutant, as compared to the WT p30 C/EBP α -BioID (Figure 3B). BioID with p30 C/EBP α -tR>L also verified the methylation-dependent interaction with the E3 ubiquitin ligase TRIM33 and the NuRD complex component GATAD2A, as also detected by PRISMA. In addition, several Myb-Muvb/DREAM complex members (LIN9, LIN37, MYBL2) were identified as p30 C/EBP α -tR>L-specific interactors, but were not detected in PRISMA.

C/EBP α isoform specific interactions detected with BioID

The PRISMA data predicted that p30 C/EBP α can still function to recruit major components of the transcriptional and epigenetic machinery, albeit with lower efficiency compared to p42 C/EBP α . To further examine the differences between the two C/EBP α isoforms, we expressed p42 and p30 C/EBP α as BioID fusions in NB4 cells to compare their BioID interactomes. The isoform-specific interactomes (Figure 4A, Table S4) confirmed the binding profiles observed in PRISMA: p42 specific interactors bound more strongly to PRISMA peptides corresponding to the N-terminal, p42 unique part of C/EBP α , while p30 specific interactors predominantly bound to PRISMA peptides corresponding to C-terminal C/EBP α regions (Figure 4B). In accordance with the PRISMA interactions, most interactors identified by *in vivo* proximity labeling were found to interact with both C/EBP α isoforms (Figure 4C). These data suggest that multi-valent interactions with different affinities may occur with distinct C/EBP α CRs, including CR1L as part of p30 C/EBP α . Overall, p42 C/EBP α -BioID and p30 C/EBP α -BioID pulldowns revealed 71 and 9 interactors that preferentially interacted with p42 and p30 C/EBP α , respectively.

Proteins differentially interacting with the p30 C/EBP α isoform and its PTMs may pose a selective vulnerability for AML cells expressing p30 C/EBP α . We therefore extracted CRISPR Cas9 knockout study derived dependency scores of the nine p30 C/EBP α specific interactors in 18 different AML cell lines using the DepMap Portal (Figure S5) (Tsherniak et al., 2017). Among the AML cell lines inspected, 9 out of 18 scored as sensitive to TFAP4 knockout (threshold <- 0.5). Two and one cell line tested were sensitive to GATA1 and BCL11A or BLM

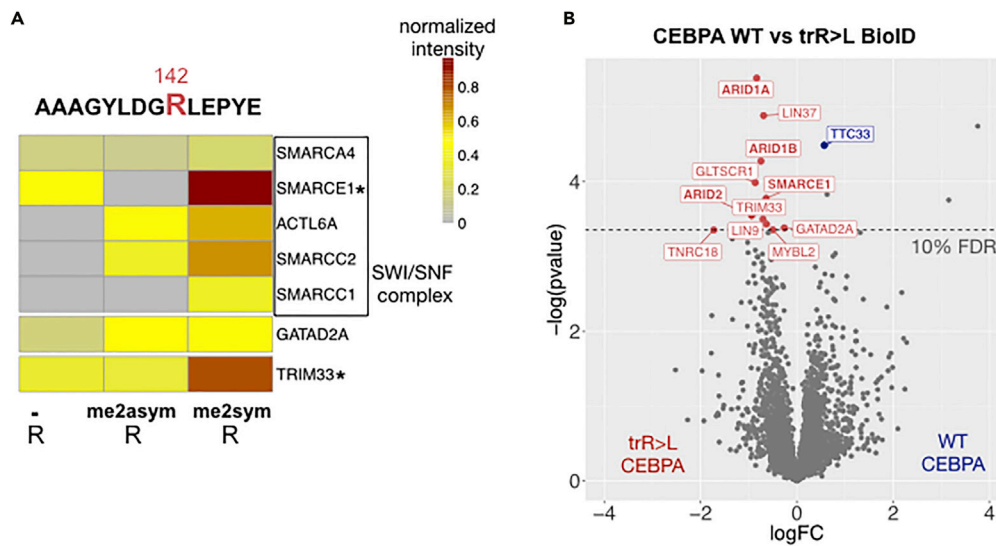


Figure 3. BAF/SWI-SNF complex subunit SMARCE1 preferentially interacts with R142 methylated CEBPA

(A) PRISMA interaction profile of proteins differentially binding to CEBPA peptides centered at R142. Peptide sequence is shown on top and methylation status of R142 is shown at the bottom. Interactors found significant (FDR 0.1) in the R142 dimethylated peptide are marked with *.

(B) BioID pull-downs with wildtype CEBPA and trR>L CEBPA were compared with a student t-test ($n = 4$). Proteins passing the significance threshold (0.1 FDR) in wildtype to mutant comparison and significant compared to controls are marked in color. Significant BAF/SWI-SNF subunits are indicated by bold letters.

See also [Figure S2](#), [Tables S3](#) and [S4](#).

knockout, respectively. The p30 C/EBP α specific binding of the BAF/SWI-SNF complex member BCL11A further highlights context-specific regulation of BAF/SWI-SNF complex interaction to C/EBP α isoforms.

To analyze connections between the C/EBP α isoform specific interactome with the transcriptome, we also performed RNA expression analysis of NB4 cell lines ectopically expressing p42 or p30 C/EBP α . We found that despite the largely overlapping interactome, the two isoforms induced differential gene expression changes ([Figure 4D](#)) that could be attributed to differential interactions with other transcription factors. Gene expression profiles were analyzed using gene set enrichment analysis (GSEA) employing immunologic and transcription factor target databases from the molecular signature database ([Subramanian et al., 2005](#)) ([Figure 4E](#)). The erythroid transcription factor GATA1 was found to interact differentially with p30 C/EBP α ; GSEA analysis detected enrichment of a GATA1 signature specifically in p30 C/EBP α expressing cells. Likewise, PPARG specifically interacts with p42 C/EBP α and p42 expressing cells also displayed significant enrichment of a previously published macrophage PPARG gene signature ([Roszler et al., 2011](#)). Data from BioID experiments indicated that EGR1 specifically interacted with p42 C/EBP α . Interestingly, we found that a gene signature based on the presence of EGR1 motifs was enriched in p30 but not p42 C/EBP α expressing cells. RNA expression levels of EGR1 were upregulated by both p42 and p30 expression. Indirect interaction of EGR1 with DNA not at EGR1 motifs, but through other CEBPs, has been described previously ([Jakobsen et al., 2013](#)) and may contribute to the differential EGR1 signature observed. Taken together, our data suggest that the specific interactions of C/EBP α isoforms with lineage defining transcription factors are implicated in co-regulation of target genes in the hematopoietic system.

DISCUSSION

In the present study, we combined peptide array screening and BioID to overcome limitations of classical immuno-affinity based interactomes of intrinsically disordered transcription factors, such as C/EBP α . PRISMA reveals both SLiM- and PTM-dependent interactions ([Dittmar et al., 2019](#); [Meyer et al., 2018](#); [Meyer and Selbach, 2020](#)) while BioID covalently biotinylates proteins that engage with C/EBP α in the living cell and is thus well suited for the detection of dynamic interactions ([Roux et al., 2012](#)). The integration of both methods fine mapped a high confidence C/EBP α interaction landscape across the C/EBP α sequence and PTM sites.

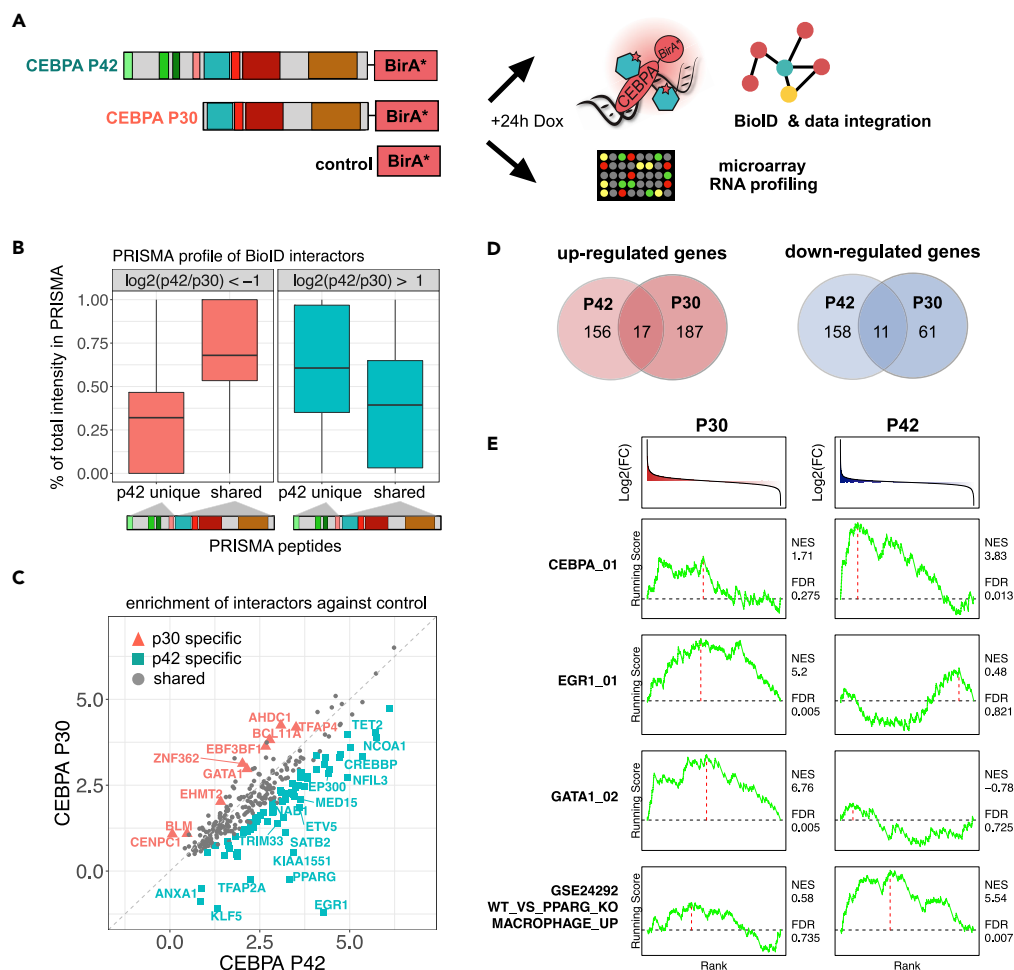


Figure 4. BioID with CEBPA p42/p30 isoforms disclose isoform-specific interactors in conjunction with PRISMA profiles

(A) BioID interaction proteomics (n = 4) and microarray RNA expression (n = 3) were performed with CEBPA isoform (p42 or p30) expressing cells.

(B) PRISMA profiles of interactors showing preference for p42 ($\log_2(p42/p30) > 1$) or p30 ($\log_2(p42/p30) < -1$) in BioID. LFQ intensities of proteins were summed across PRISMA peptides corresponding to exclusively p42 or both isoforms. The resulting numbers were divided by the total LFQ intensity of each protein across all PRISMA peptides. PTM-modified peptides were omitted from the calculations.

(C) Relative enrichment of CEBPA interactors against the control, p42 is plotted against p30. Proteins marked in color passed 0.1 FDR threshold in a direct comparison.

(D) Overlap of up- and downregulated genes as detected by microarray gene expression profiling (comparison to BirA* cells, FDR < 0.05, absolute fold change (FC) > 1).

(E) Induced gene expression changes were subjected to ssGSEA analysis. Normalized enrichment score (NES) and FDR of informative gene sets are displayed next to running score line plots. The running score was calculated with Kolmogorov-Smirnov (K-S) running sum statistics.

See also [Figure S5](#), [Table S4](#).

The core interactome of 137 proteins is highly interconnected and, in addition to known C/EBP α interactors that operationally represent positive controls, we also discovered novel associations of C/EBP α with proteins involved in gene expression and epigenetic regulation, chromosome organization, RNA processing, and DNA replication. The majority of C/EBP α interactions were nevertheless detected in only one of the two datasets. Some of the unique C/EBP α interactors detected by BioID may require more complex, simultaneously occurring, multi-site interactions or multiple induced fit processes and were missed in PRISMA. Discrepancies may also relate to restriction of BioID to proximal interactions, the absence of suitable

biotinylation sites, or stability during the labeling period. PRISMA, on the other hand, may readily detect distal, secondary interactors, such as in large protein complexes.

PRISMA revealed major hotspots of protein interactions in C/EBP α that strongly correlated with data derived from the related transcription factor C/EBP β (Dittmar et al., 2019; Leutz et al., 2011). The interactors shared between C/EBP α and C/EBP β may help to explain the partially redundant functions of both proteins (Chen et al., 2000; Hirai et al., 2006; Jones et al., 2002). Many of the co-regulators identified also displayed multiple interactions with several conserved regions that represent subdivisions of previously defined trans-regulatory regions found within the C/EBP family (Leutz et al., 2011). The same conserved regions scored highly as molecular recognition features (MoRF; Figure 1B) that may undergo induced folding and transient disorder-to-order transition during contact with partner proteins (Oldfield et al., 2005). For example, the region CR3,4 of C/EBP ϵ was previously shown to fold into two short orthogonal amphipathic helical regions on interaction with the TAZ2 domain of CBP (Bhaumik et al., 2014). Likewise, CBP/p300 was found to interact with PRISMA peptides covering CR3,4 of C/EBP α , in concordance with homologous regions in C/EBP β (Dittmar et al., 2019). Interestingly, CR3,4 in C/EBP α and C/EBP ϵ are separated by only few amino acids, whereas species-specific IDRs separate both CRs in C/EBP β , suggesting structural spatial flexibility and independent, yet combinatorial functions of CR3,4.

Many regulatory proteins involved in signaling, gene expression, and epigenetics harbor IDRs and PTMs that determine their function and connectivity (Dyson and Wright, 2005, 2016). Multivalent, promiscuous interactions of transcription factors with co-regulatory proteins have been observed before and may relate to context dependent contacts during dynamic gene regulatory processes (Brzovic et al., 2011; Clark et al., 2018; Vojnic et al., 2011). This concept is in accordance with the dynamic nature of SLiMs and may reflect multi-modal regulation with a rapid exchange of alternative interaction partners (Dyson and Wright, 2016; Ivarsson and Jemth, 2019). Modular transactivation domains in conjunction with multivalency are thought to participate in or to initiate biomolecular condensates that involve dynamic, “fuzzy” interactions with multiple co-regulators in interaction hubs (Bojja et al., 2018; Brzovic et al., 2011; Chong et al., 2018; Hahn, 2018; Martin and Holehouse, 2020; Tuttle et al., 2018). Remarkably, the C/EBP α primary structure shows a very high degree of “fuzziness” with strong predictions as initiator regions of liquid-liquid phase separation in the N-terminus (Figure 1B, red line), while the PRISMA interaction hotspots largely coincide within regions that show maxima of MoRF predictions (Figure 1B, blue line) (Horvath et al., 2020; Malhis et al., 2016).

Our data show that PTMs in C/EBP α may orchestrate multi-modal functions of C/EBP α by modulating interactions with the components of transcriptional and epigenetic machinery. The comparison of C/EBP α WT and the R142L methylation mimicry mutant by proximity labeling confirmed the differential interaction with BAF/SWI-SNF components, as detected by PRISMA. These data are consistent with previous findings showing that BAF/SWI-SNF interacts with CR1L (Muller et al., 2004; Pedersen et al., 2001). The newly discovered R142 methylation-dependent differential interaction of BAF/SWI-SNF will help to conceive hypothesis driven approaches to explore arginine methyltransferase-dependent epigenetic downstream events.

Data presented here further demonstrate that most of the C/EBP α interactors bind to both C/EBP α isoforms, whereas a subset of 71 and 9 proteins preferentially interacted with the p42 and p30 C/EBP α isoform, respectively. Many of the shared C/EBP α interactors showed diminished signal strength in p30 C/EBP α BioID, supporting the concept of p30 as a “weak” C/EBP α variant with relatively few exclusive binding partners. This view is supported by the fact that defective myelopoiesis in the absence of C/EBP α was largely rescued by p30 C/EBP α , although p30, in the absence of p42 C/EBP α , eventually elicits AML (Bereshchenko et al., 2009; Kirstetter et al., 2008a, 2008b). Interestingly, several of the p30 C/EBP α -specific binders (TFAP4, GATA1, BCL11A) affect the survival of AML cell lines. The p30 C/EBP α specific interaction with GATA1 may further hint at a role at the branchpoint of erythroid/myeloid commitment in replicative multi-potential progenitors (Drissen et al., 2019), whereas p42 C/EBP α specific interactors, such as EGR1 or PPAR γ , are important regulators of myeloid differentiation (Chinetti et al., 1998; Krishnaraju et al., 2001; Lefterova et al., 2008, 2010; Mildner et al., 2017; Nguyen et al., 1993; Roszer et al., 2011; Tontonoz et al., 1994).

In summary, the cross-validated myeloid C/EBP α interaction map presented in this study may serve as a resource for further exploration of the biological importance of individual and combinatorial SLiM and PTM functions of C/EBP α . Beyond the C/EBP α , β interactomes, the integration of PRISMA and BioID

approaches may help to explore the linear and PTM-dependent interactomes of many other important intrinsically disordered proteins involved in cell signaling and cell fate determination.

Limitations of the study

Both, the PRISMA and BioID C/EBP α interactomes were generated with the human acute promyelocytic leukemia cell line NB4. The BioID labeling required a 24 hr period and interactions with short-lived proteins may be under-represented. Changing cell lines and/or biotin ligases with higher turnover rates may help to identify additional interaction partners.

STAR★METHODS

Detailed methods are provided in the online version of this paper and include the following:

- KEY RESOURCES TABLE
- RESOURCE AVAILABILITY
 - Lead contact
 - Materials availability
 - Data and code availability
- EXPERIMENTAL MODEL AND SUBJECT DETAILS
 - Cell lines
 - CEBPA BioID NB4 cell lines
- METHOD DETAILS
 - NB4 induction
 - Nuclear extract preparation
 - Protein interaction screen on a peptide matrix
 - LC MS/MS
 - BioID experiments
 - Targeted MS analysis of R142 methylation
 - Raw data processing with MaxQuant
 - Data analysis of mass spec data
 - Microarray
 - GSEA of microarray data
- QUANTIFICATION AND STATISTICAL ANALYSIS

SUPPLEMENTAL INFORMATION

Supplemental information can be found online at <https://doi.org/10.1016/j.isci.2021.102686>.

ACKNOWLEDGMENTS

We thank Tommaso Mari and Marieluise Kirchner for scientific discussions. E.R. was supported by a fellowship of the Berlin School of Integrated Oncology (BSIO). The project was partially supported by a grant to A.L., DFG, LE 770/4-2. Parts of figures were created with BioRender.com.

AUTHOR CONTRIBUTIONS

Conceptualization, A.L., G.D., E.R., D.P.; Methodology, A.L., E.R., E.K.L., V.S.; Investigation and Validation, E.R., V.S., E.K.L.; Resources, G.D., A.L., P.M., U.R., N.N., P.N.; Data curation, E.R., K.Z., A.L.; Writing original draft, E.R.; Writing, review and editing, E.R., A.L., E.K.L., P.M.; Visualization, E.R., A.L.; Supervision, project administration, and funding acquisition, A.L. (ORCID: 0000-0001-8259-927X), G.D. (ORCID: 0000-0003-3647-8623), P.M. (ORCID: 0000-0002-2245-528X).

DECLARATION OF INTERESTS

The authors declare no conflicts of interest.

Received: January 16, 2021

Revised: May 17, 2021

Accepted: May 30, 2021

Published: June 25, 2021

REFERENCES

- Avellino, R., and Delwel, R. (2017). Expression and regulation of C/EBPalpha in normal myelopoiesis and in malignant transformation. *Blood* 129, 2083–2091.
- Barbie, D.A., Tamayo, P., Boehm, J.S., Kim, S.Y., Moody, S.E., Dunn, I.F., Schinzel, A.C., Sandy, P., Meylan, E., Scholl, C., et al. (2009). Systematic RNA interference reveals that oncogenic KRAS-driven cancers require TBK1. *Nature* 462, 108–112.
- Bereshchenko, O., Mancini, E., Moore, S., Bilbao, D., Månsson, R., Luc, S., Grover, A., Jacobsen, S.E.W., Bryder, D., and Nerlov, C. (2009). Hematopoietic stem cell expansion precedes the generation of committed myeloid leukemia-initiating cells in C/EBPα mutant AML. *Cancer Cell* 16, 390–400.
- Bhaumik, P., Davis, J., Tropea, J.E., Cherry, S., Johnson, P.F., and Miller, M. (2014). Structural insights into interactions of C/EBP transcriptional activators with the Taz2 domain of p300. *Acta Crystallogr. D Biol. Crystallogr.* 70, 1914–1921.
- Boija, A., Klein, I.A., Sabari, B.R., Dall'Agnese, A., Coffey, E.L., Zamudio, A.V., Li, C.H., Shrinivas, K., Manteiga, J.C., Hannett, N.M., et al. (2018). Transcription factors activate genes through the phase-separation capacity of their activation domains. *Cell* 175, 1842–1855.e16.
- Brzovic, P.S., Heikaus, C.C., Kisselev, L., Vernon, R., Herbig, E., Pacheco, D., Warfield, L., Littlefield, P., Baker, D., Klevit, R.E., et al. (2011). The acidic transcription activator Gcn4 binds the mediator subunit Gal11/Med15 using a simple protein interface forming a fuzzy complex. *Mol. Cell* 44, 942–953.
- Bushell, K.M., Sollner, C., Schuster-Boeckler, B., Bateman, A., and Wright, G.J. (2008). Large-scale screening for novel low-affinity extracellular protein interactions. *Genome Res.* 18, 622–630.
- Chatr-Aryamontri, A., Oughtred, R., Boucher, L., Rust, J., Chang, C., Kolas, N.K., O'Donnell, L., Oster, S., Theesfeld, C., Sellam, A., et al. (2017). The BioGRID interaction database: 2017 update. *Nucleic Acids Res.* 45, D369–D379.
- Chen, S.S., Chen, J.F., Johnson, P.F., Muppala, V., and Lee, Y.H. (2000). C/EBPbeta, when expressed from the C/ebpalpha gene locus, can functionally replace C/EBPalph in liver but not in adipose tissue. *Mol. Cell. Biol.* 20, 7292–7299.
- Chinetti, G., Griglio, S., Antonucci, M., Torra, I.P., Delerive, P., Majd, Z., Fruchart, J.C., Chapman, J., Najib, J., and Staels, B. (1998). Activation of proliferator-activated receptors alpha and gamma induces apoptosis of human monocyte-derived macrophages. *J. Biol. Chem.* 273, 25573–25580.
- Chong, S., Dugast-Darzacq, C., Liu, Z., Dong, P., Dailey, G.M., Cattoglio, C., Heckert, A., Banala, S., Lavis, L., Darzacq, X., et al. (2018). Imaging dynamic and selective low-complexity domain interactions that control gene transcription. *Science* 361, eaar2555.
- Cirilli, M., Bereshchenko, O., Ermakova, O., and Nerlov, C. (2017). Insights into specificity, redundancy and new cellular functions of C/EBPa and C/EBPb transcription factors through interactome network analysis. *Biochim. Biophys. Acta Gen. Subj.* 1861, 467–476.
- Clark, S., Myers, J.B., King, A., Fiala, R., Novacek, J., Pearce, G., Heierhorst, J., Reichow, S.L., and Barbar, E.J. (2018). Multivalency regulates activity in an intrinsically disordered transcription factor. *Elife* 7, 1–28.
- Cox, J., and Mann, M. (2008). MaxQuant enables high peptide identification rates, individualized p.p.b.-range mass accuracies and proteome-wide protein quantification. *Nat. Biotechnol.* 26, 1367–1372.
- Dignam, J.D., Lebovitz, R.M., and Roeder, R.G. (1983). Accurate transcription initiation by RNA polymerase II in a soluble extract from isolated mammalian nuclei. *Nucleic Acids Res* 11, 1475–1489. <https://doi.org/10.1093/nar/11.5.1475>.
- Dittmar, G., Hernandez, D.P., Kowenz-Leutz, E., Kirchner, M., Kahlert, G., Wesolowski, R., Baum, K., Knoblich, M., Hofstatter, M., Muller, A., et al. (2019). PRISMA: protein interaction screen on peptide matrix reveals interaction footprints and modifications- dependent interactome of intrinsically disordered C/EBPbeta. *iScience* 13, 351–370.
- Drissen, R., Thongjuea, S., Theilgaard-Monch, K., and Nerlov, C. (2019). Identification of two distinct pathways of human myelopoiesis. *Sci. Immunol.* 4, eaau7148.
- Dunker, A.K., Brown, C.J., Lawson, J.D., Iakoucheva, L.M., and Obradovic, Z. (2002). Intrinsic disorder and protein function. *Biochemistry* 41, 6573–6582.
- Dyson, H.J., and Wright, P.E. (2005). Intrinsically unstructured proteins and their functions. *Nat. Rev. Mol. Cell. Biol.* 6, 197–208.
- Dyson, H.J., and Wright, P.E. (2016). Role of intrinsic protein disorder in the function and interactions of the transcriptional coactivators CREB-binding protein (CBP) and p300. *J. Biol. Chem.* 291, 6714–6722.
- Fasan, A., Haferlach, C., Alpermann, T., Jeromin, S., Grossmann, V., Eder, C., Weissmann, S., Dicker, F., Kohlmann, A., Schindela, S., et al. (2014). The role of different genetic subtypes of CEBPA mutated AML. *Leukemia* 28, 794–803.
- Giamb Bruno, R., Grebien, F., Stukalov, A., Knoll, C., Panyavsky, M., Rudashevskaya, E.L., Colinge, J., Superti-Furga, G., and Bennett, K.L. (2013). Affinity purification strategies for proteomic analysis of transcription factor complexes. *J. Proteome Res.* 12, 4018–4027.
- Grebien, F., Vedadi, M., Getlik, M., Giamb Bruno, R., Avellino, R., Skucha, A., Vittori, S., Kuznetsova, E., Baryte-lovejoy, D., Li, F., et al. (2016). Pharmacological targeting of the Wdr5-MLL interaction in C/EBPα N-terminal leukemia. *Nat. Chem. Biol.* 11, 571–578.
- Hahn, S. (2018). Phase separation, protein disorder, and enhancer function. *Cell* 175, 1723–1725.
- Hirai, H., Zhang, P., Dayaram, T., Hetherington, C.J., Mizuno, S., Imanishi, J., Akashi, K., and Tenen, D.G. (2006). C/EBPbeta is required for 'emergency' granulopoiesis. *Nat. Immunol.* 7, 732–739.
- Horvath, A., Miskei, M., Ambrus, V., Vendruscolo, M., and Fuxreiter, M. (2020). Sequence-based prediction of protein binding mode landscapes. *Plos Comput. Biol.* 16, e1007864.
- Huang, da W., Sherman, B.T., and Lempicki, R.A. (2009). Systematic and integrative analysis of large gene lists using DAVID bioinformatics resources. *Nat. Protoc.* 4, 44–57.
- Ivarsson, Y., and Jemth, P. (2019). Affinity and specificity of motif-based protein-protein interactions. *Curr. Opin. Struct. Biol.* 54, 26–33.
- Jakobsen, J.S., Waage, J., Rapin, N., Bisgaard, H.C., Larsen, F.S., and Porse, B.T. (2013). Temporal mapping of CEBPA and CEBPB binding during liver regeneration reveals dynamic occupancy and specific regulatory codes for homeostatic and cell cycle gene batteries. *Genome Res.* 23, 592–603.
- Jones, L.C., Lin, M.L., Chen, S.S., Krug, U., Hofmann, W.K., Lee, S., Lee, Y.H., and Koeffler, H.P. (2002). Expression of C/EBPbeta from the C/ebpalpha gene locus is sufficient for normal hematopoiesis in vivo. *Blood* 99, 2032–2036.
- Kirstetter, P., Schuster, M.B., Bereshchenko, O., Moore, S., Dvinge, H., Kurz, E., Theilgaard-Mönch, K., Månsson, R., Pedersen, T.A., and Pabst, T. (2008a). Modeling of C/EBPα mutant acute myeloid leukemia reveals a common expression signature of committed myeloid leukemia-initiating cells. *Cancer Cell* 13, 299–310.
- Kirstetter, P., Schuster, M.B., Bereshchenko, O., Moore, S., Dvinge, H., Kurz, E., Theilgaard-Mönch, K., Månsson, R., Pedersen, T.A., Pabst, T., et al. (2008b). Modeling of C/EBPalpha mutant acute myeloid leukemia reveals a common expression signature of committed myeloid leukemia-initiating cells. *Cancer Cell* 13, 299–310.
- Kowenz-Leutz, E., Pless, O., Dittmar, G., Knoblich, M., and Leutz, A. (2010). Crosstalk between C/EBPbeta phosphorylation, arginine methylation, and SWI/SNF/Mediator implies an indexing transcription factor code. *EMBO J.* 29, 1105–1115.
- Krishnaraju, K., Hoffmann, B., and Liebermann, D.A. (2001). Early growth response gene 1 stimulates development of hematopoietic progenitor cells along the macrophage lineage at the expense of the granulocyte and erythroid lineages. *Blood* 97, 1298–1305.
- Lefterova, M.I., Steger, D.J., Zhuo, D., Qatanani, M., Mullican, S.E., Tuteja, G., Manduchi, E., Grant, G.R., and Lazar, M.A. (2010). Cell-specific determinants of peroxisome proliferator-activated receptor gamma function in adipocytes and macrophages. *Mol. Cell. Biol.* 30, 2078–2089.
- Lefterova, M.I., Zhang, Y., Steger, D.J., Schupp, M., Schug, J., Cristancho, A., Feng, D., Zhuo, D., Stoeckert, C.J., Jr., Liu, X.S., et al. (2008). PPARgamma and C/EBP factors orchestrate adipocyte biology via adjacent binding on a genome-wide scale. *Genes Dev.* 22, 2941–2952.
- Leutz, A., Pless, O., Lappe, M., Dittmar, G., and Kowenz-Leutz, E. (2011). Crosstalk between phosphorylation and multi-site arginine/lysine methylation in C/EBPs. *Transcription* 2, 3–8.
- Lin, L.I., Chen, C.Y., Lin, D.T., Tsay, W., Tang, J.L., Yeh, Y.C., Shen, H.L., Su, F.H., Yao, M., Huang,

- S.Y., et al. (2005). Characterization of CEBPA mutations in acute myeloid leukemia: most patients with CEBPA mutations have biallelic mutations and show a distinct immunophenotype of the leukemic cells. *Clin. Cancer Res.* 11, 1372–1379.
- Malhis, N., Jacobson, M., and Gsponer, J. (2016). MoRFchibi SYSTEM: software tools for the identification of MoRFs in protein sequences. *Nucleic Acids Res.* 44, W488–W493.
- Martin, E.W., and Holehouse, A.S. (2020). Intrinsically disordered protein regions and phase separation: sequence determinants of assembly or lack thereof. *Emerg. Top Life Sci.* 4, 307–329.
- Meerbrey, K.L., Hu, G., Kessler, J.D., Roarty, K., Li, M.Z., Fang, J.E., Herschkowitz, J.I., Burrows, A.E., Ciccio, A., Sun, T., et al. (2011). The pINDUCER lentiviral toolkit for inducible RNA interference in vitro and in vivo. *Proc. Natl. Acad. Sci. U S A* 108, 3665–3670.
- Meyer, K., Kirchner, M., Uyar, B., Cheng, J.Y., Russo, G., Hernandez-Miranda, L.R., Szymorska, A., Zauber, H., Rudolph, I.M., Willnow, T.E., et al. (2018). Mutations in disordered regions can cause disease by creating dileucine motifs. *Cell* 175, 239–253.e17.
- Meyer, K., and Selbach, M. (2020). Peptide-based interaction proteomics. *Mol. Cell Proteomics* 19, 1070–1075.
- Mildner, A., Schonheit, J., Giladi, A., David, E., Lara-Astiaso, D., Lorenzo-Vivas, E., Paul, F., Chappell-Maor, L., Priller, J., Leutz, A., et al. (2017). Genomic characterization of murine monocytes reveals C/EBPβ transcription factor dependence of Ly6C(−) cells. *Immunity* 46, 849–862.e7.
- Muller, C., Calkhoven, C.F., Sha, X., and Leutz, A. (2004). The CCAAT enhancer-binding protein alpha (C/EBPα) requires a SWI/SNF complex for proliferation arrest. *J. Biol. Chem.* 279, 7353–7358.
- Nguyen, H.Q., Hoffmanliebermann, B., and Liebermann, D.A. (1993). The Zinc finger transcription factor Egr-1 is essential for and restricts differentiation along the macrophage lineage. *Cell* 72, 197–209.
- Oldfield, C.J., Cheng, Y., Cortese, M.S., Romero, P., Uversky, V.N., and Dunker, A.K. (2005). Coupled folding and binding with alpha-helix-forming molecular recognition elements. *Biochemistry* 44, 12454–12470.
- Pabst, T., Mueller, B.U., Zhang, P., Radomska, H.S., Narravula, S., Schnitter, S., Behre, G., Hiddemann, W., and Tenen, D.G. (2001). Dominant-negative mutations of CEBPA, encoding CCAAT/enhancer binding protein-alpha (C/EBPα), in acute myeloid leukemia. *Nat. Genet.* 27, 263–270.
- Pedersen, T.Å., Kowenz-leutz, E., Leutz, A., and Nerlov, C. (2001). Cooperation between C/EBPα TBP/TFIIB and SWI/SNF recruiting domains is required for adipocyte differentiation. *Genes Development* 15, 3208–3216.
- Perez-Riverol, Y., Csordas, A., Bai, J., Bernal-Linares, M., Hewapathirana, S., Kundu, D.J., Inuganti, A., Griss, J., Mayer, G., Eisenacher, M., et al. (2019). The PRIDE database and related tools and resources in 2019: improving support for quantification data. *Nucleic Acids Res.* 47, D442–D450.
- Perkins, J.R., Diboun, I., Dessailly, B.H., Lees, J.G., and Orengo, C. (2010). Transient protein-protein interactions: structural, functional, and network properties. *Structure* 18, 1233–1243.
- Pino, L.K., Searle, B.C., Bollinger, J.G., Nunn, B., MacLean, B., and MacCoss, M.J. (2020). The Skyline ecosystem: Informatics for quantitative mass spectrometry proteomics. *Mass Spectrom. Rev.* 39, 229–244.
- Rappsilber, J., Ishihama, Y., and Mann, M. (2003). Stop and go extraction tips for matrix-assisted laser desorption/ionization, nanoelectrospray, and LC/MS sample pretreatment in proteomics. *Anal. Chem.* 75, 663–670.
- Ritchie, M.E., Phipson, B., Wu, D., Hu, Y., Law, C.W., Shi, W., and Smyth, G.K. (2015). Limma powers differential expression analyses for RNA-seq and microarray studies. *Nucleic Acids Res.* 43, e47.
- Roszer, T., Menendez-Gutierrez, M.P., Lefterova, M.I., Alameda, D., Nunez, V., Lazar, M.A., Fischer, T., and Ricote, M. (2011). Autoimmune kidney disease and impaired engulfment of apoptotic cells in mice with macrophage peroxisome proliferator-activated receptor gamma or retinoid X receptor alpha deficiency. *J. Immunol.* 186, 621–631.
- Roux, K.J., Kim, D.I., Raida, M., and Burke, B. (2012). A promiscuous biotin ligase fusion protein identifies proximal and interacting proteins in mammalian cells. *J. Cell Biol.* 196, 801–810.
- Sabari, B.R., Dall’Agnese, A., and Young, R.A. (2020). Biomolecular condensates in the nucleus. *Trends Biochem. Sci.* 45, 961–977.
- Seldeen, K.L., McDonald, C.B., Deegan, B.J., and Farooq, A. (2008). Coupling of folding and DNA-binding in the bZIP domains of Jun-Fos heterodimeric transcription factor. *Arch. Biochem. Biophys.* 473, 48–60.
- Shannon, P., Markiel, A., Ozier, O., Baliga, N.S., Wang, J.T., Ramage, D., Amin, N., Schwikowski, B., and Ideker, T. (2003). Cytoscape: a software environment for integrated models of biomolecular interaction networks. *Genome Res.* 13, 2498–2504.
- Subramanian, A., Tamayo, P., Mootha, V.K., Mukherjee, S., Ebert, B.L., Gillette, M.A., Paulovich, A., Pomeroy, S.L., Golub, T.R., Lander, E.S., et al. (2005). Gene set enrichment analysis: a knowledge-based approach for interpreting genome-wide expression profiles. *Proc. Natl. Acad. Sci. U S A* 102, 15545–15550.
- Szklarczyk, D., Franceschini, A., Wyder, S., Forslund, K., Heller, D., Huerta-Cepas, J., Simonovic, M., Roth, A., Santos, A., Tsafou, K.P., et al. (2015). STRING v10: protein-protein interaction networks, integrated over the tree of life. *Nucleic Acids Res.* 43, D447–D452.
- Tompa, P. (2012). Intrinsically disordered proteins: a 10-year recap. *Trends Biochem. Sci.* 37, 509–516.
- Tontonoz, P., Hu, E., Graves, R.A., Budavari, A.I., and Spiegelman, B.M. (1994). mPPAR gamma 2: tissue-specific regulator of an adipocyte enhancer. *Genes Dev.* 8, 1224–1234.
- Tsherniak, A., Vazquez, F., Montgomery, P.G., Weir, B.A., Kryukov, G., Cowley, G.S., Gill, S., Harrington, W.F., Pantel, S., Krill-Burger, J.M., et al. (2017). Defining a cancer dependency map. *Cell* 170, 564–576.e516.
- Tsukada, J., Yoshida, Y., Kominato, Y., and Auron, P.E. (2011). The CCAAT/enhancer (C/EBP) family of basic-leucine zipper (bZIP) transcription factors is a multifaceted highly-regulated system for gene regulation. *Cytokine* 54, 6–19.
- Tuttle, L.M., Pacheco, D., Warfield, L., Luo, J., Ranish, J., Hahn, S., and Kleiv, R.E. (2018). Gcn4-Mediator specificity is mediated by a large and dynamic fuzzy protein-protein complex. *Cell Rep.* 22, 3251–3264.
- Uversky, V.N., Oldfield, C.J., and Dunker, A.K. (2005). Showing your ID: intrinsic disorder as an ID for recognition, regulation and cell signaling. *J. Mol. Recognit.* 18, 343–384.
- van der Lee, R., Buljan, M., Lang, B., Weatheritt, R.J., Daughdrill, G.W., Dunker, A.K., Fuxreiter, M., Gough, J., Gsponer, J., Jones, D.T., et al. (2014). Classification of intrinsically disordered regions and proteins. *Chem. Rev.* 114, 6589–6631.
- Vojnic, E., Mourao, A., Seizl, M., Simon, B., Wenzek, L., Larivière, L., Baumli, S., Baumgart, K., Meisterernst, M., Sattler, M., et al. (2011). Structure and VP16 binding of the Mediator Med25 activator interaction domain. *Nat. Struct. Mol. Biol.* 18, 404–409.
- Ward, J.J., Sodhi, J.S., McGuffin, L.J., Buxton, B.F., and Jones, D.T. (2004). Prediction and functional analysis of native disorder in proteins from the three kingdoms of life. *J. Mol. Biol.* 337, 635–645.
- Wright, P.E., and Dyson, H.J. (1999). Intrinsically unstructured proteins: re-assessing the protein structure-function paradigm. *J. Mol. Biol.* 293, 321–331.
- Zaret, K.S., and Carroll, J.S. (2011). Pioneer transcription factors: establishing competence for gene expression. Parameters affecting transcription factor access to target sites in chromatin Initiating events in chromatin: pioneer factors bind first. *Genes Development*, 2227–2241.
- Zhang, P., Iwasaki-Arai, J., Iwasaki, H., Fenyes, M.L., Dayaram, T., Owens, B.M., Shigematsu, H., Levantini, E., Huettner, C.S., Leksrom-Himes, J.A., et al. (2004). Enhancement of hematopoietic stem cell repopulating capacity and self-renewal in the absence of the transcription factor C/EBP alpha. *Immunity* 21, 853–863.

STAR★METHODS

KEY RESOURCES TABLE

REAGENT or RESOURCE	SOURCE	IDENTIFIER
Chemicals, peptides, and recombinant proteins		
NeutrAvidin™ Agarose	ThermoFisher Scientific	Cat# 29201
Deposited data		
Raw and analyzed MS data	This paper	PRIDE: PXD022903
Microarray data	This paper	ArrayExpress: E-MTAB-9947
Human protein reference database	UniProt	https://www.uniprot.org/proteomes/UP000005640
Experimental models: Cell lines		
NB4 cell line	Leibniz Institute DSMZ- German Collection of Microorganisms and Cell Culture	ACC 207
CEBPA BioID NB4 cell lines	This paper	
Oligonucleotides		
Primer BirA Ligase PCR forward: CGCGGATCCAGCGGTGGAAGTGG TGGCCTGAAGGACAACACCGTG Reverse: TGCTCTAGACTCGAGTTATT TATCGTC	This paper	
Recombinant DNA		
BirA plasmid	(Bushell et al., 2008)	Addgene Plasmid #64395
pInducer21 GFP lentiviral vector	(Meerbrey et al., 2011)	Clontech #3044
Software and algorithms		
MaxQuant Version 1.5.2.8	(Cox and Mann, 2008)	https://www.maxquant.org/maxquant/
R studio desktop Version 1.3.1093	R studio	https://www.rstudio.com/
R Version 3.6.3	The R Project for Statistical Computing	https://www.r-project.org/
Cytoscape Version 3.7.1	(Shannon et al., 2003)	https://cytoscape.org/
Transcriptome Analysis Console (TAC 4.0)	ThermoFisher Scientific	
single sample gene set enrichment analysis tool (ssGSEA)	(Barbie et al., 2009)	https://github.com/broadinstitute/ssGSEA2.0
LIMMA package	(Ritchie et al., 2015)	https://bioconductor.org/packages/release/bioc/html/limma.html
Other		
Custom PepSpot cellulose membranes	JPT Peptide Technologies GmbH	

RESOURCE AVAILABILITY

Lead contact

Further information and requests for resources and reagents should be directed to and will be fulfilled by the lead contact, Achim Leutz (aleutz@mdc-berlin.de)

Materials availability

This study did not generate new unique reagents.

Data and code availability

The mass spectrometry proteomics data and search results generated during this study have been deposited to the ProteomeXchange Consortium via the PRIDE partner repository ([Perez-Riverol et al., 2019](#)) with

the dataset identifier PXD022903. Microarray data generated during this study have been deposited in the ArrayExpress database at EMBL-EBI (www.ebi.ac.uk/arrayexpress) under accession number E-MTAB-9947.

EXPERIMENTAL MODEL AND SUBJECT DETAILS

Cell lines

NB4 cells (RRID:CVCL_0005) were acquired from Leibniz Institute DSMZ- German Collection of Microorganisms and Cell Culture, Germany (DSMZ no.: ACC 207). Cells were cultivated in a humidified incubator at 37°C, 5% CO₂ in RPMI1640. For metabolic labeling, NB4 cells were grown in SILAC RPMI1640 supplemented with 10% dialyzed FCS, 100 mg/ml penicillin-streptomycin, 25mM HEPES, 28 µg/ml L-arginine and 48.67 µg/ml L-lysine (light) 13C615N2 (heavy lysine) or L-lysine D4 (medium heavy lysine).

CEBPA BioID NB4 cell lines

The rat C/EBPα p30 3L mutant (R140; 147; 154 mutated to leucine) was generated using the QuickChange Site Directed Mutagenesis Kit according to the manufacturer's protocol (Agilent #200519). The BirA Ligase containing plasmid was purchased (Addgene #64395). The BirA Ligase was cloned in frame to the C/EBPα C-terminus using BamHI and XhoI restriction sites. PCR primer: 5'-CGCGGATCCAGCGGTG-GAAGTGGTGGCCTGAAGGACAACACCGTG and 3'- TGCTCTAGACTCGAGTTATTTATCGTC. The C/EBPα p42, p30 or p30 R3L-BirA Ligase fragments were cloned into the pENTRY2B vector (Clontech #3064) using BamHI and XhoI restriction sites and subsequently introduced into the pInducer21 GFP lentiviral vector (Clontech #3044) using the Gateway LR Clonase™ II cloning kit (ThermoFisher Scientific #11791-020). Viral supernatants were obtained from Lenti-X 293T cells (Clontech #632180) transfected with either pInducer21 GFP lentiviral vector or pInducer21 GFP constructs containing either p42, p30 WT-BirA Ligase, p30 R3L-BirA Ligase, or pInducer21 GFP-BirA ligase only using Lenti-X Packing Single Shots (Clontech #631275) according to the manufacturer's protocol. NB4 cells were centrifuged (1 h, 900g) with infectious supernatant collected 72 h after transfection and 8 µg/mL hexadimethrine bromide and left for recovery overnight. GFP positive NB4 cells were sorted twice using an Aria II sorter (Becton Dickinson) three days after infection.

METHOD DETAILS

NB4 induction

NB4 cells were briefly treated with differentiation inducing agents prior to harvesting. SILAC labeled NB4 cells were seeded during exponential growth in SILAC media supplemented with 2µM all-trans-retinoic acid (ATRA; heavy), 50nM Tetradeanoylphorbol-acetate (TPA; medium heavy) or solvent only (light). Cells were harvested after 12h (ATRA and solvent only treated cells) or 6h (TPA treated cells) and nuclear extracts were prepared as described.

Nuclear extract preparation

Nuclear extracts from NB4 cells were prepared as described previously (Dignam et al., 1983) with slight modifications. NB4 cells were harvested by centrifugation at 1000g, 4 min at 4°C and washed twice with icecold PBS. Packed cell volume (pcv) was estimated and cells were resuspended in 5xpcv of ice-cold hypotonic buffer (10mM HEPES pH 7.5, 10mM NaCl, 3mM MgCl₂) supplemented with protease inhibitors. Cells were incubated on ice for 5 min, followed by addition of dodecyl-β-D-maltosid (DDM) to a final concentration of 0.05%. The sample was vortexed briefly and immediately centrifuged for 5 min at 600g, 4°C. The cytosolic fraction was removed and the nuclei were washed with 20xpcv hypotonic buffer (5 min, 600g, 4°C). The supernatant was removed and the nuclei were washed with 20xpcv PBS (5 min, 600g, 4°C). The nuclei were extracted with 2/3xpcv of high salt buffer (20mM HEPES pH 7.5, 400mM NaCl, 1mM EDTA pH 8, 1mM EGTA pH 8, 20% glycerol, 1mM DTT) supplemented with protease inhibitors while shaking on a tubeshaker at 4°C for 20 min at 750 rpm. Nuclear extracts were cleared by centrifugation at 18000g for 20 min at 4°C and the buffer was exchanged to membrane binding buffer (20mM HEPES pH 7.5, 400mM NaCl, 1mM EDTA pH 8, 1mM EGTA pH 8, 25% glycerol, 1mM DTT) by gel filtration with PD MidiTrap G10 columns (GE healthcare) according to instructions of manufacturers.

Protein interaction screen on a peptide matrix

Custom PepSpot cellulose membranes were ordered from JPT Peptide Technologies (Germany) and PRISMA was performed as described before (Dittmar et al., 2019) with slight adaptations. All washing and incubation steps were performed at 4°C on a rocking platform set to 700 rpm. Membranes were wetted

in membrane binding buffer for 15 min, followed by a blocking step with 1 mg/ml yeast tRNA in membrane binding buffer for 10 min. Membranes were washed 5 x for 5 min with membrane binding buffer and incubated with nuclear extracts on ice for 30 min. The protein extract was removed and the membranes were washed 3 x 5 min with membrane binding buffer. The individual peptide spots were punched out with a 2mm biopsy puncher and placed into single wells of a 96-well plate containing 20 μ l denaturation buffer (6M urea, 2M thiourea, 10mM HEPES pH 8). The samples were digested in solution on a PAL robot system. In brief, proteins were reduced with 1mM tris(2-carboxyethyl)phosphine for 30 min followed by alkylation with 5mM 2-chloroacetamide for 20 min. To each sample 0.5 μ g of sequencing grade lysyl endopeptidase (LysC, FUJIFILM Wako Pure Chemical Corporation) was added. Samples were digested for 2 h before being diluted with four volumes of 50mM ammonium-bi-carbonate and continuation of the digestion overnight at room temperature. Digested samples were acidified with formic acid and desalted with C18 stage tips as described before (Rappsilber et al., 2003). Briefly, 3 disks of 3MTM EmporeTM C18 material were placed into 200 μ l pipet tips and resulting stage tips were conditioned with 50 μ l methanol, followed by 100 μ l elution buffer (50% acetonitrile/0.1% formic acid) and 100 μ l 0.1% formic acid. Acidified samples were loaded, washed three times with 100 μ l 0.1% formic acid and eluted with 50 μ l elution buffer. All steps were performed in a tabletop centrifuge (2 min, 2000g). Samples were dried in a vacuum concentrator prior to LC MS/MS analysis.

LC MS/MS

Desalted and dried peptides were resuspended in MS sample buffer (3% acetonitrile/0.1% formic acid) and separated online with an Easy-nLCTM1200 coupled to a Q exactive+ or a Q exactive HF-X mass spectrometer equipped with an orbitrap electrospray ion source (all Thermo Fisher Scientific). Samples were separated on line on a 20 cm reverse-phase column (inner diameter 75 μ m) packed in house with 3 μ m C18-Reprosil beads with a linear gradient ramping from 3% to 76% acetonitrile. PRISMA samples were separated with a 1h gradient and MS data was acquired on a Q exactive+ in data dependent acquisition mode with a top10 method. Full scan MS spectra were acquired at a resolution of 70000 in the scan range from 300 to 1700 m/z, automated gain control (AGC) target value of $1e^6$ and maximum injection time of 120ms. MS/MS spectra were acquired at a resolution of 17500, AGC target of $1e^5$ and maximum IT of 60 ms. Ions were isolated with a 2 m/z isolation window and normalized collision energy was set to 26. Unassigned charge states and single charged precursors were excluded from fragmentation and dynamic exclusion was set to 20s. BioID pulldowns were separated on with a 2 h gradient and MS data was acquired on a Q exactive HF-X in data dependent acquisition mode with a top20 method. Full scan MS spectra were acquired at a resolution of 60000 in the scan range from 350 to 1700 m/z, automated gain control (AGC) target value was set to $3e^6$ and maximum injection time to 10ms. MS/MS spectra were acquired at a resolution of 30000, AGC target of $1e^5$ and maximum IT of 86 ms. Ions were isolated with a 1.6 m/z isolation window and normalized collision energy was set to 26. Unassigned charge states and ions with a charge state of one, seven or higher were excluded from fragmentation and dynamic exclusion was set to 30s.

BioID experiments

NB4 stable cell lines were grown in RPMI supplemented with tetracycline free FCS. Cells were seeded in exponential growth phase in media supplemented with 1mM biotin and 1 μ g/ml doxycycline in quadruplicates. Cells were harvested after 24h by centrifugation and washed twice with cold PBS. Cell pellets were resuspended in lysis buffer (50 mM tris-HCl (pH 7.2), 150 mM, NaCl, 1% NP-40, 1 mM EDTA, 1 mM EGTA, 0.1% SDS, 1% sodium deoxycholate) supplemented with cOmpleteTM Mini EDTA-free Protease Inhibitor Cocktail (Roche) and incubated on ice for 20 min. Samples were sonicated with a probe sonicator for 5 pulses and centrifuged for 20 min at 4°C, 20 000g. For each pulldown (1x 15 cm dish), 80 μ l neutravidin-agarose bead slurry (Thermo Fisher Scientific) was used. Beads were washed twice in lysis buffer and added to the protein extracts. The samples incubated rotating at 4°C for 2.5 h. Beads were washed 3x with lysis buffer, 1x with 1M KCl, 1x 2M Urea in 50mM Tris pH8 and 3x with 50mM Tris pH8. Washing buffers were kept on ice and each washing step was performed with 1ml, inverting the tube 5 times and then centrifuging for 1 min at 2000g to pellet the beads. Washed beads were resuspended in 80 μ l ureabuffer (2M urea, 50mM Tris pH7.5, 1mM DTT) supplemented with 5 μ g/ml trypsin (sequencing grade, Promega) and incubated 1 h at RT on a tubeshaker at 1000rpm. The supernatant was transferred into a fresh tube, the beads washed twice with 60 μ l 2M urea/50mM Tris pH7.5 and the supernatant combined with the supernatant from the previous step. Residual beads were removed by an additional centrifugation (1 min, 5000g) and sample transfer step. Eluted proteins were reduced with 4mM DTT for 30 min on a tubeshaker (RT, 1000 rpm). Proteins were alkylated with 10mM 2-Iodoacetamide in the dark for 45 min (RT,

1000 rpm) and digested over night with 0.5 µg trypsin at RT on a thermoshaker at 700 rpm. For an AspN digest, 0.5 µg of trypsin and 0.5 µg sequencing grade endoproteinase AspN (Promega) were added to the sample. Following overnight digestion, samples were acidified by adding TFA and desalted with stage tips.

Targeted MS analysis of R142 methylation

Synthetic heavy peptide standards with the sequence DGRLEPLEYER and DGR[me]LEPLEYER labeled at the C-terminus with heavy arginine [Arg10] were custom synthesized by JPT Peptide Technologies (Germany). CEBPA BioID pull-downs were digested with AspN and trypsin and desalted as described. Samples were resuspended in MS sample buffer containing 100 fmol/µl of synthetic heavy peptides. Parallel reaction monitoring (PRM) measurements were acquired on a Q exactive HF-X mass spectrometer coupled to an Easy-nLC™ 1200 HPLC system. Peptides were separated on a 60 min gradient ramping from 2% to 76% acetonitrile. Data acquisition mode cycled between a Top1 MS/data dependent MS2 and data independent measurement of an inclusion list that included the m/z of the synthetic heavy peptides as well as their light counterparts coming from the sample. Resolution of MS2 for data independent acquisition was 60000 with an AGC target of 1e6, 200 ms maximum IT, 0.7 m/z isolation window and NCE of 27. PRM data was analyzed with Skyline (Pino et al., 2020). Identity of peptides was verified by comparison with the elution profile and fragmentation spectrum of heavy peptide standards.

Raw data processing with MaxQuant

Mass spectrometry raw files were processed with MaxQuant (version 1.5.2.8) (Cox and Mann, 2008) searching against a human protein database containing isoforms downloaded from UniProt (June 2017) and a database including common contaminants. Fixed modifications were set to carbamidomethylation of cysteines and variable modifications were set to methionine oxidation and N-terminal acetylation. For BioID experiments, lysine biotinylation was added as an additional variable modification. Depending on digestion mode (trypsin or LysC only), enzyme specificity was selected with a maximum of 2 missed cleavages per peptide. The initial allowed mass deviation of the precursor ion was up to 6 ppm and 20 ppm for fragments. False-discovery rate was set to 1% on protein and peptide level. For SILAC measurements, the requantify option was enabled and minimum ratio count was set to 2. For LFQ analysis, the match between run and fast LFQ options was used with default settings.

Data analysis of mass spec data

Statistical analysis of the dataset was performed using R-statistical software package (version 3.4.1). The protein group's output file from MaxQuant was filtered for contaminants, reverse hits and proteins only identified by site. Minimum peptide count for SILAC and LFQ data was at least 2 peptides per protein group. For LFQ datasets, proteins were filtered by detection in at least 3 replicates of the same sample and missing values were imputed from a distribution at the detection limit of the mass spectrometer. For this purpose, a normal distribution was created for each run, with a mean 1.8 standard deviations away from the observed mean and a standard deviation of 0.3 x the observed standard deviation. LFQ data was analysed with a two-sample moderated t-test (Limma package) and p-values were corrected for multiple testing with the Benjamini-Hochberg procedure. The significance cutoff of CEBPA interactors was enrichment against both controls (BirA* only and cells not treated with doxycycline) with an FDR <0.05. For isoform and tR>L mutant specific interactors, threshold was enrichment against both controls with an FDR <0.05 and FDR <0.1 in the pairwise comparison of isoforms and mutants. Interactors overlapping between PRISMA and BioID or BioID and literature (STRING and BioGrid database, Grebien et al., Giambruno et al.) were visualized with the STRING app built into cytoscape (v3.7.1) (Shannon et al., 2003). Known interaction (experimentally validated or deposited in databases with a score >0.5) were visualized as edges. Interactors not connected by any edges were removed from Figure 2C (12 proteins). GO term analysis of interactors was performed with DAVID functional annotation tool (version 6.8) (Huang et al., 2009). PRISMA data was analysed with a two-sample moderated t-test (Limma package), creating a specific control group for each peptide that contained all other peptides excluding peptides with a sequence overlap ≥50%. P-values were corrected for multiple testing with Benjamini-Hochberg procedure, significance cut off was <0.1 FDR. To obtain binding profiles of interactors, LFQ intensities of significant proteins were normalized between 0 and 1 across all PRISMA peptides.

Microarray

Cells were harvested at exponential growth phase and seeded at 0.5×10^6 cells/ml in RPMI supplemented with or without $1 \mu\text{g}/\mu\text{l}$ doxycycline as independent biological triplicates. After 24 hr, cells were harvested via centrifugation (1200 g, 5 min, 4°C) and washed once with 1x icecold PBS. Total RNA was extracted with the RNeasy Mini Kit (Qiagen) following manufacturer's instructions. DNA was removed with the DNase Max Kit (Qiagen) following manufacturer's instructions. RNA integrity was assessed using a Fragment Analyzer system and a standard sensitivity RNA kit. All RQN scores were above 9.1. RNA expression analysis was performed with Affymetrix Human ClariomS® microarray using the WT Plus Reagent kit (ThermoFisher Scientific). As starting material, 100ng of total RNA was used and RNA was prepared for hybridization with the GeneChip® Whole Transcript (WT) PLUS Reagent Kit (ThermoFisher Scientific) following manufactures instructions. CEL files were processed using the standard Transcriptome Analysis Console (TAC 4.0) software. Expression values were automatically normalized and summarized using SST-RMA method. Only mRNAs with \log_2 expression above 6 in at least one sample were considered for further analysis. Statistical analysis was performed using LIMMA package of R/Bioconductor and p-values were adjusted using Benjamini-Hochberg's FDR.

GSEA of microarray data

Gene expression changes induced by CEBPA isoforms were calculated by comparing microarray data from NB4 cells expressing CEBPA (P42 or P30) against BirA* expressing cells. Averaged \log_2 fold changes were used as input for the single sample gene set enrichment analysis (ssGSEA) analysis tool (Barbie et al., 2009) implemented in R (<https://github.com/broadinstitute/ssGSEA2.0>) using standard parameters. Data was analyzed employing immunologic and transcription factor target gene sets from the molecular signature database (Subramanian et al., 2005). The running score displayed in Figure 4 was calculated with Kolmogorov-Smirnov running sum statistics.

QUANTIFICATION AND STATISTICAL ANALYSIS

Statistical analyses of the data were performed using the R-statistical software package (version 3.4.1). The type of statistical tests used is annotated in figure legends and described in detail in the method details sections. Statistical parameters (n, mean, significance level) are reported in the figures and legends or in corresponding supplemental tables.